Water and Wastewater, Vol. , No. , pp:

Development of an Individual Hydro-Edge Flow Direction Tool in ArcGIS Environment: A Novel Extension for Looped Water Distribution Networks Using LiDAR-Derived Elevation Data

Mohamad Almasinia[1*], Wan Muhd Aminuddin Wan Hussin[2], Mohd. Sanusi S. Ahamad[2]

1. Assist. Prof., Dept. of Geography, Faculty of Humanities, Payame Noor University, Tehran, Iran (Corresponding Author) almasi@pnu.ac.ir
2. Retired Prof., formerly of School of Civil Engineering, University Sains Malaysia, Engineering Campus, 14300 Nibong Tebal, Pulau Pinang, Malaysia

https://doi.org/10.22093/wwj.2026.557085.3542 **Original Paper**

Abstract

Accurate determination of flow direction in water distribution networks is a fundamental prerequisite for hydraulic modeling, leakage detection, valve isolation, and network maintenance. While ArcGIS Utility Network Analyst provides robust tools for tree-like (branched) networks, it fundamentally fails to assign determinate flow direction in looped configurations due to the absence of inherent downstream topology. This study addresses this critical gap by developing a novel custom extension, the "Individual Flow Direction Tool," which integrates high-resolution LiDAR-derived digital elevation models with geometric network intelligence to assign flow direction on a per-hydro-edge basis. The research methodology comprises four integrated phases. First, a comprehensive geodatabase was designed incorporating 12 feature classes (pipelines, valves, fittings, hydrants, reservoirs, meter-boxes) with predefined subtypes, attribute domains, and connectivity rules. Second, a 1m-resolution DEM and subsequent 3D surface model were generated from airborne LiDAR data (decimeter accuracy). Third, Z-values were extracted for all junction endpoints using the "Extract Values to Points" tool. Fourth, the IFD Tool-developed as a custom ArcGIS add-in-was programmed to evaluate each edge individually based on the comparative Z-values of its two terminal junctions, iteratively propagating flow determination through complex loop systems. The tool was validated against field-verified flow data from Syarikat Air Johor Holdings for 14 interconnected loops comprising 3.7 km of PVC pipelines (D=150mm, C=150) in Taman Mutiara Rini, Malaysia. The IFD Tool successfully assigned flow direction to 100% of network edges. Comparative analysis revealed 79% agreement (1,428 out of 1,807 edges) between LiDAR-based flow assignments and SAJH field data, with 21% disagreement primarily concentrated within loop interiors rather than source-sink trunks. Hardy-Cross verification confirmed hydraulic balance in all disagreed edges, demonstrating that the Hardy-Cross method can yield multiple valid flow solutions for a given looped network. Consequently, the 21% disagreement does not indicate a methodological flaw; rather, it reflects the existence of multiple hydraulically balanced flow regimes. The SAJH field data captures the specific operational state influenced by undocumented interventions (e.g., booster pumps, partially closed valves), while the IFD Tool provides the topographically natural baseline. This research presents the first documented ArcGIS extension specifically designed for looped-network flow assignment using topographic intelligence. The IFD Tool transforms WDN management by enabling scientific, reproducible flow determination independent of subjective engineering judgment. Based on this specific case study (flat terrain, uniform PVC pipes), the methodology is estimated to reduce utility expenditure on flow direction field verification by 70-80%. However, further validation across diverse topographic conditions and pipe materials is required to generalize this estimate.

Keywords:
Water Distribution Network, Flow Direction, ArcGIS Extension, Geometric Network, LiDAR, Looped Network, Utility Network Analyst, Hardy-Cross Method.

Received: June 13, 2025
Revised: Sep. 8, 2025
Accepted: Oct. 5, 2025

To cite this article:
Almasinia, M., Wan Hussin, W. M. A., Ahamad, M. S. S., 2026. Development of an individual hydro-edge flow direction tool in ArcGIS environment: a novel extension for looped water distribution networks using LiDAR-derived elevation data. *Water and Wastewater*, (In press).
https://doi.org/10.22093/wwj.2026.557085.3542.

Use your device to scan and read the article online

1. Introduction

1.1. Background and problem statement

Water Distribution Networks[1] constitute critical urban infrastructure, responsible for delivering potable water under adequate pressure and flow conditions. A fundamental yet persistently challenging parameter in WDN modeling and management is the determination of flow direction within individual pipelines (Mays, 2010; Walski, 2006). Unlike transportation networks where direction is imposed by regulatory signage, utility networks exhibit commodity flow that is physically determined by pressure gradients, elevation differences, and network topology (Pickus et al., 2005). Hydraulic modeling plays a crucial role in pressure and leakage management of urban WDNs (Eskandaripour et al., 2025).

The Geographic Information System[2], particularly ArcGIS, has become the industry standard for WDN asset management. ESRI's Utility Network Analyst extension provides sophisticated tools for network tracing, upstream/downstream analysis, and valve isolation (Zeiler, 1999). However, a critical functional limitation persists: the automatic flow direction algorithm in ArcGIS fails to compute determinate flow for looped network configurations. This limitation stems from the software's reliance on explicit source-sink declarations; in a true loop with multiple potential flow paths and no designated sink, the algorithm returns "indeterminate flow" or arbitrarily assigns direction based on digitized orientation (Abdel-Khalik and Sadowski, 1997).

This deficiency has significant practical consequences. Water utility engineers confronted with looped networks are forced to resort to one of three suboptimal strategies: (1) manual flow assignment based on experiential judgment, (2) expensive field deployment of acoustic Doppler or tracer studies, or (3) complete reliance on standalone hydraulic models (EPANET, WaterGEMS) disconnected from the corporate GIS database. All three approaches introduce subjectivity, data redundancy, and operational latency.

1.2. Research gap and novelty

Extensive literature review confirms that while substantial research has addressed WDN optimization (Zheng et al., 2011; Samani and Zanganeh, 2010), hydraulic calibration (Jolly et al., 2014), and GIS integration (Rangzan and Mehrabi, 2008; Zhang, 2006), no published study has specifically targeted the automation of flow direction assignment in looped networks within the native ArcGIS environment. Previous GIS-WDN integrations either: (a) limited analysis to tree-type distribution mains (Varma et al., 1997); (b) exported GIS data to external hydraulic solvers without bidirectional flow (Tospornsampan et al., 2007); or (c) relied on assumed flow patterns from design drawings rather than topographic reality (Eusuff and Lansey, 2003). Several studies have focused on network renewal planning using historical event data (Salehi et al., 2024). Additionally, artificial neural networks have been successfully applied for leakage detection in water distribution systems (Attari and Faghfour Maghrebi, 2018).

It is important to distinguish the Individual Flow Direction[3] Tool from hydraulic simulators such as EPANET and WaterGEMS. While those software packages solve full mass and energy conservation equations to compute flow rates, pressures, and flow directions under given demand scenarios, they require extensive input data (nodal demands, pump curves, valve settings) and are designed for steady-state or extended-period simulation.

In contrast, the IFD Tool is a custom extension within the ArcGIS environment that directly operates on the geometric network of the GIS database. Its primary purpose is to resolve a specific, well-documented limitation of ArcGIS Utility Network Analyst: the inability to assign determinate flow direction to looped configurations (referred to as "indeterminate flow" in ESRI documentation). The IFD Tool assigns flow directions solely based on LiDAR[4]-derived elevation data, requiring no operational parameters. It provides a topographically natural baseline that can be used for initial network setup, data quality control, or as a preprocessing step before detailed hydraulic simulation.

Thus, the claim of "first extension for looped networks" refers specifically to the native ArcGIS environment, not to the hydraulic simulation field. No previous ArcGIS extension has automated flow direction assignment in loops using LiDAR-derived Z-values.

The present research introduces three distinct novelties:

First, we develop a purpose-built ArcGIS extension (IFD Tool) that executes edge-by-edge flow determination using LiDAR-extracted Z-values, fundamentally circumventing ArcGIS's algorithmic constraint on loops. Recent advances in LiDAR-based feature extraction (Arav and Filin, 2022; Bartmiński et al., 2023) have demonstrated the feasibility of semi-automated linear feature detection from point cloud data, providing methodological foundations for our approach.

Beyond general feature extraction, several recent studies have specifically utilized high resolution LiDAR derived DEMs for automatic drainage and channel network extraction. Arghavanian and Leloğlu, (2024) introduced a curvature based method with cross section tracking to extract irrigation channels from LiDAR data in flat plains. Lidberg et al., (2023) applied deep learning to airborne laser scanning data for mapping drainage ditches in forested landscapes at a regional scale. Meirose et al., (2024) demonstrated that LiDAR derived

[1] Water Distribution Networks (WDNs)
[2] Geographic Information System (GIS)
[3] Individual Flow Direction (IFD)
[4] Light Detection and Ranging (LiDAR)

DEMs significantly improve stream delineation accuracy compared to coarser products like InSAR. Tiwari et al., (2025) compared satellite versus aerial (UAV/LiDAR) data for urban waterlogging assessment and found that LiDAR provides superior microtopographic detail. Additionally, Vakily, (2024) analyzed uncertainty in catchment characteristics derived from different LiDAR based DEMs, highlighting the importance of DEM source selection.

Second, we establish a formal decision logic (Equation 1) that models flow direction as a ternary state function of comparative endpoint elevation, explicitly recognizing the hydraulic validity of level-ground and counter-gradient flows induced by pumping.

Third, we provide the first published validation of LiDAR-derived Z-values for sub-meter pipeline junction elevation extraction, demonstrating decimeter accuracy sufficient for gravity-fed network analysis in flat urban terrain.

1.3. Objectives

The specific objectives of this research are:

- To design and implement a geometric network-enabled geodatabase capable of storing and managing LiDAR-extracted Z-values as intrinsic junction attributes.
- To develop the IFD Tool algorithm and deploy it as a functional ArcGIS add-in.
- To validate the IFD Tool against field-verified flow data using both direct comparison (agreement percentage) and hydraulic balancing (Hardy-Cross method) (Cross, 1936).
- To quantify the sources and patterns of flow disagreement between topographic inference and operational reality.

2. Materials and methods

2.1. Study area description

The research was conducted in Taman Mutiara Rini, Johor Bahru, Malaysia (1°30′57″–1°31′52″ N, 103°37′24″–103°38′52″ E). This 2.8 km² residential catchment was selected for three characteristics critical to the research objectives:

(1) Complex loop topology: Unlike simple branched distribution systems, Taman Mutiara Rini contains 14 interconnected hydraulic loops ranging from 3 to 12 edges per loop. This complexity provides a rigorous testbed for evaluating flow determination in non-trivial configurations.

(2) Flat topography: The area exhibits minimal relief (elevation range 22–31 m AHD), representing the most challenging condition for elevation-based flow assignment. Successful flow determination in flat terrain demonstrates the sensitivity of decimeter-accurate LiDAR.

(3) Data availability: Comprehensive asset data (pipeline centrelines, valve locations, fitting types, meter-box positions) and field-verified flow direction records were provided by Syarikat Air Johor Holdings[1], the regional water authority.

It should be noted that the study area is a newly developed residential suburb. Based on the project's procurement and installation standards, a single nominal diameter of 150 mm was uniformly adopted for the main reticulation pipes to streamline construction and reduce logistical complexity. This practice is supported by the concept of 'diameter uniformity' in WDN design, which is recognized as a practical approach for improving network reliability and flow uniformity in newly developed flat urban areas (Creaco et al., 2014). Additionally, the Hazen-Williams coefficient C=150 is the standard recommended value for new, clean PVC pipes, as documented in multiple engineering references (Onsite Installer, 2026; Engineering Toolbox, n.d.; Access Engineering Library, n.d.).

Fig. 1 presents the overall research methodology flowchart. The methodology comprises four main phases: (1) geodatabase design and geometric network construction; (2) LiDAR data processing, DEM[2] generation, and 3D surface modeling; (3) Z-value extraction for network junctions; and (4) development and validation of the IFD Tool using Hardy-Cross verification.

2.2. Data acquisition

2.2.1. Vector datasets

SAJH supplied 12 shapefile layers representing complete WDN infrastructure:

SAJH supplied 12 shapefile layers representing complete WDN infrastructure. The vector datasets included transmission mains (n=47, PVC, D=150 mm), reticulation pipes (n=1,346, PVC, D=100-150 mm), service connections (n=1,223, PE, D=25 mm), and junction features including valves (n=312), fittings (n=894), fire hydrants (n=56), reservoirs (n=2), and meter-boxes (n=1,126). All vector data were originally captured at 1:1,000 scale with reported positional accuracy ±0.3 m.

2.2.2. LiDAR data

Airborne LiDAR data were acquired in March 2014 using an Optech ALTM Gemini scanner mounted on a fixed-wing platform. The key acquisition parameters included a flying height of 1,200 m AGL, a scan angle of ±18°, and a pulse rate of 100 kHz. The point density was 4.2 points/m² for the first return and 3.8 points/m² after ground classification. The reported vertical accuracy was 0.09 m RMSE, which was independently verified as 0.11 m RMSE against 32 GPS[3] ground control points. The horizontal accuracy was 0.18 m.

[1] Syarikat Air Johor Holdings (SAJH)
[2] Digital Elevation Model (DEM)
[3] Global Positioning System (GPS)

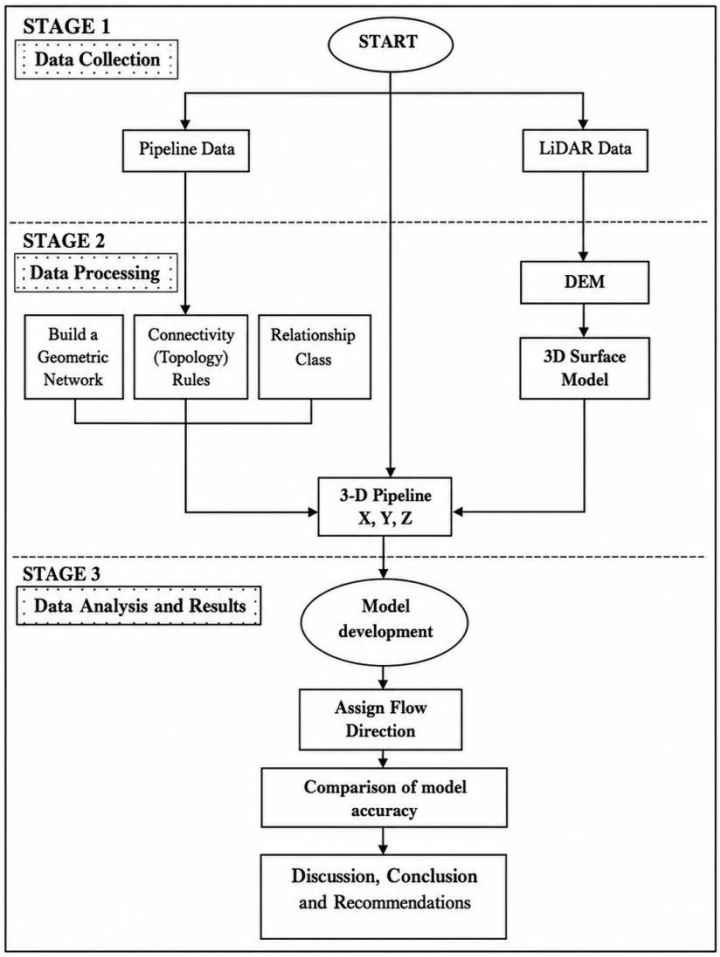

Fig. 1. Research flow chart of determination of flow direction

2.3. Geodatabase architecture

A file geodatabase was constructed as the central data repository (Fig. 1). The architecture follows ESRI's best practices for utility network implementation but introduces two novel enhancements specific to flow direction analysis.

2.3.1. Feature dataset organization

All 12 feature classes were consolidated within a single feature dataset ("WaterNetwork") to enable topological integration. Feature classes were categorized into three functional groups:

Group A – Edge Features:
- Transmission_Main (simple edge)
- Reticulation_Pipe (complex edge; enabling service taps without feature fragmentation)
- Service_Pipe (simple edge)

Group B – Junction Features:
- Reservoir (source role; cardinality constraint: 1 per network)
- Valve (junction; enabled/disabled state)
- Fitting (complex junction; representing tees, reducers, elbows)
- Hydrant (junction)
- Meter_Box (sink role; cardinality constraint: ≥1 per service area)

Group C – Annotation/Support:
- Dimension_Features
- Relationship_Classes

The organization of feature datasets and feature classes is illustrated in Fig. 2.

2.3.2. Domain and subtype implementation

To enforce data integrity and streamline attribute entry, coded value domains were established for critical fields: Subtypes were implemented for the Reticulation_Pipe feature class to differentiate hydraulic behavior across pipe diameters without creating multiple feature classes. The domain and subtype configuration parameters are summarized in Table 1.

2.3.3. Geometric network construction

The geometric network was generated using the ArcGIS Geometric Network Wizard with the following specifications:

Network name: WD_GeometricNet

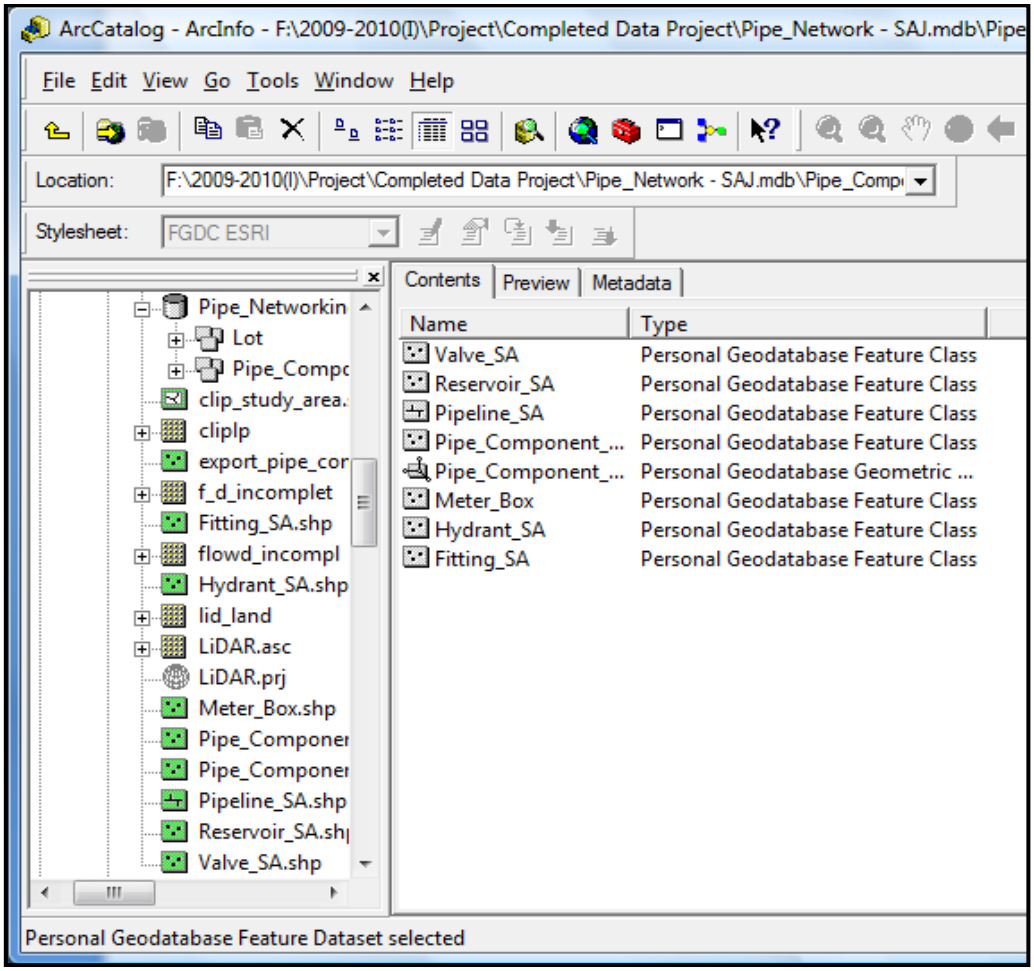

Fig. 2. Geodatabase architecture and feature dataset organization

Table 1. Domain and subtype configuration parameters

Feature class	Field name	Domain values	Default value	Subtypes
Reticulation_Pipe	Material	PVC (1); Mild steel (2); HDPE (3)	PVC (1)	Main; Secondary; service
Reticulation_Pipe	Diameter_mm	100; 150; 200; 250	150	-
Valve	Status	Enabled (1); Disabled (0)	Enabled (1)	-
Fitting	Fitting_type	Tee (1); Reducer (2); Elbow_45 (3); Elbow_90 (4); Coupling (5)	-	-
Meter_box	Customer_type	Residential (1); Commercial (2); Industrial (3)	Residential (1)	-

Snap tolerance: 0.1 m (critical for capturing true connectivity from source data with positional inconsistencies)
Complex edge configuration: Reticulation_Pipe designated as complex edge; all other edges simple
Orphan junction behavior: Enabled; orphan junctions subsequently merged with nearest fitting feature class

Connectivity rules were programmatically enforced to prevent illogical connections (e.g., direct reservoir-to-meter box without intervening pipe). A partial rule set is illustrated in Fig. 3. The domain and subtype configuration parameters are summarized in Table 1.

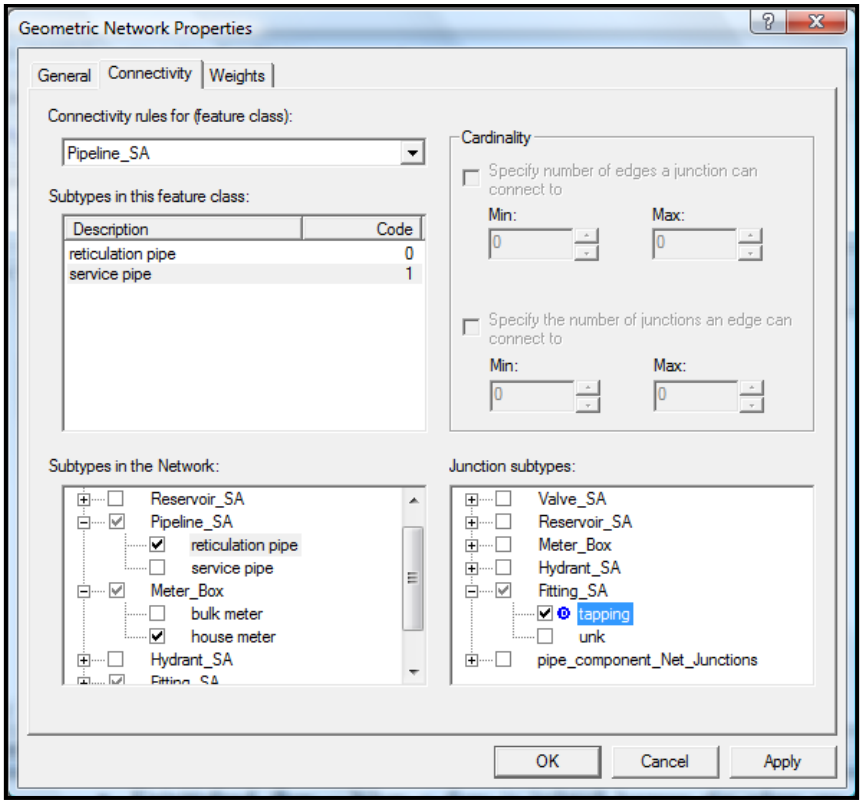

Fig. 3. Geometric network connectivity rules (schematic)

Table 2. Descriptive statistics of LiDAR-derived junction elevations (n = 4,823)

Statistic	Value (m)
Minimum	22.14
Maximum	31.87
Mean	26.93
Median	26.81
Standard Deviation	2.34
25th Percentile	25.02
75th Percentile	28.79

2.4. LiDAR processing and elevation extraction

2.4.1. DEM and 3D surface model generation

Classified ground returns (.las format) were processed in ArcGIS 9.3 using the LAS Dataset toolbox. Processing workflow:

- Point filtering: Retained class 2 (ground) points only
- Outlier removal: Statistical filtering (3σ threshold) eliminated anomalous elevation values
- Interpolation: Triangulated Irregular Network (TIN) generation using natural neighbors algorithm
- Raster conversion: TIN to raster at 1.0 m cell resolution, bilinear resampling
- Hydrologic conditioning: Sink filling (≤0.15 m depth threshold) to prevent artificial depressions

The resulting DEM exhibited mean error = +0.03 m, RMSE = 0.11 m relative to 32 independent GPS checkpoints, confirming decimeter accuracy suitable for urban flow analysis.

2.4.2. Junction Z-value extraction

All junction feature vertices (n=4,823) were extracted as point feature classes. The "Extract Values to Points" tool (Spatial Analyst) was executed to sample DEM pixel values at each junction location. Extracted Z-values were written to a dedicated attribute field ("Z_LiDAR", float, precision 0.01 m).

The descriptive statistics of extracted elevations are presented in Table 2. The flow direction agreement between IFD and SAJH is summarized in Table 3.

Table 3. Pipe properties for sample loop (Loop 1)

Pipe ID	Diameter (mm)	Length (m)	Relative roughness	Hazen-Williams C	r (N-s²/m⁸)
P1.2	150	248	0.000043	150	3.99E-004
P1.6	150	243	0.000043	150	3.91E-004
P2.3	150	79	0.000043	150	1.27E-004
P3.4	150	96	0.000043	150	1.55E-004
P4.5	150	105	0.000043	150	1.69E-004
P5.6	150	7	0.000043	150	1.13E-005

Table 4. Flow direction agreement matrix (IFD vs. SAJH)

Network type	Number of edges	Agreed	Disagreed	Agreement (%)
Trunk mains	374	351	23	94%
Loop interior	1,433	1,077	356	71%
Total	1,807	1,428	379	79%

The extracted Z-values ranged from 22.14 m to 31.87 m, with a mean of 26.93 m and a standard deviation of 2.34 m (detailed descriptive statistics are summarized in Table 4 of the Results section).

2.5. IFD tool: algorithm and implementation

2.5.1. Theoretical framework

The IFD Tool operates on a fundamental hydraulic principle: in a gravity-dominated system, water flows from higher hydraulic head to lower head. At the pipeline scale, with negligible velocity head and friction losses small relative to elevation differential, the terminal junction with greater elevation serves as the effective source for that edge.

We formalize this as a ternary decision rule:

$$\begin{cases} Z_{HL} > Z_{LL} & \text{IFD is Normal} \\ Z_{HL} = Z_{LL} & \text{IFD is Level Ground} \\ Z_{HL} < Z_{LL} & \text{IFD is Opposite} \end{cases} \quad (1)$$

Where,

Z_{HL} = Higher Level Elevation; IFD = Individual Flow Direction;

Z_{LL} = Lower Level Elevation;

Z is height value; HL is higher level; and LL is lower level.

LiDAR-extracted elevations of the two terminal junctions

Flow direction is stored in the geometric network as either "with digitized direction" or "against digitized direction"

It is important to note that the IFD Tool assumes a gravity-dominated flow regime. The "Counter-Gradient" case (Z1 < Z2) does not automatically imply that the flow direction is incorrect; rather, it signals a deviation from the natural topographic gradient. Such edges are precisely where pumping or external pressure sources may override gravity, and they are flagged for further investigation.

2.5.2. Algorithm pseudocode

The iterative procedure for loop balancing is presented in Algorithm 1. The IFD algorithm executes the following sequential logic:

INPUT: Geometric Network G with edge set E and junction set J

Junction attribute Z_LiDAR

Edge attribute Flow_Direction (initialized as Null)

FOR EACH edge e IN E:

ID_J1= e.FromJunction

ID_J2= e.ToJunction

Algorithm 1. Hardy-Cross iterative method for loop balancing

Step	Description
Input	Pipe length Lk, diameter Dk, and roughness coefficient Ck for each pipe k in the network.
Output	Determination of flow balance (inflow = outflow) in the water pipeline network system.
1	Calculate head-loss for each pipe Hk using the Hazen-Williams equation: $Hk = Lk \cdot \frac{10.67Q^{1.85}}{C^{1.85}D^{4.87}}$ Define inflow, outflow, and an initial flow direction assumption for each junction.
2	Identify each closed loop Lm in the system, where m is the number of closed pipeline loops.
3	Assume an initial flow direction in each loop (e.g., clockwise head-loss, CWH, and counter- clockwise head-loss, CCWH), ensuring that inflow equals outflow at each junction.
4	Compute the total clockwise head loss in the loop: ∑CWH−∑CCWH. Estimate the required change in flow (ΔQ) using Equation (3.2): $\Delta Q = \frac{\sum rQn}{L\sum nrQn}$
5	Apply the flow correction: If the change of flow (ΔQ) is positive, add it to all pipes in the loop in the counter-clockwise direction; if negative, add it in the clockwise direction.
6	Repeat from Step 3 until the change in flow (ΔQ) for all loops is within a satisfactory tolerance range (e.g., < 0.001 L/s).
7	Verify the final balance: If ∑CWH=∑CCWH (within tolerance), the flow for the loop is balanced and correct. Otherwise, re-evaluate the initial assumptions.

```
    Z1=J[ID_J1].Z_LiDAR
    Z2=J[ID_J2].Z_LiDAR

    IF Z1 > Z2 THEN:
        e.Flow_Direction="J1→J2"  // With digitized direction
    ELSE IF Z1 < Z2 THEN:
        e.Flow_Direction="J2→J1"  // Against digitized direction
    ELSE: // Z1==Z2 (within 0.05m tolerance)
        e.Flow_Direction="Indeterminate (Level)"
    END IF
    // Special handling for loops with multiple edges
    IF e is member of loop L AND count(edges in L) > 1 THEN:
        // Phase 1: Identify the highest and lowest junctions in the loop
        H = max(Z[edges in L])
        L = min(Z[edges in L])
        // Phase 2: Propagate direction outward from H to L
        FOR propagation step = 1 TO (len(L)-1):
            Assign direction for edges connecting decreasing Z values
        END FOR
    END IF
END FOR
OUTPUT: Geometric Network with complete Flow_Direction attribute
```

2.5.3. Implementation architecture

The IFD Tool was developed as a dynamic-link library[1] using ArcObjects SDK for.NET Framework 3.5, compiled in Visual C 2018. Key implementation components:

ICommand subclass: "FlowDirectionTool" – initiates the extension from ArcMap toolbar

ITool subclass: "SelectEdgeTool" – enables interactive single-edge assignment

BatchProcessor class: Executes algorithm across entire network or user-defined selection set

FlowDirectionSolver class: Core computational engine implementing Equation (1) logic

The tool registers as a custom toolbar button within ArcMap, accessible via View → Toolbars → "IFD Flow Direction". Upon execution, the tool iterates through all edges in the active geometric network, writes flow direction values to a new attribute field ("IFD_Direction"), and updates the geometric network display symbology to reflect flow arrows.

2.6. Validation protocol

2.6.1. Field data reference

SAJH provided digital network files containing authoritative flow direction records. These records represent the consolidated knowledge of as-built engineering drawings, operational observations (valve status, pressure readings), historical maintenance records, and field technician verification. The SAJH flow direction dataset served as the reference standard for accuracy assessment.

2.6.2. Accuracy metrics

Primary validation metric: Percentage Agreement (PA) calculated as:

[1] Dynamic-Link Library[1] (DLL)

$$PA = \frac{Nagree}{Ntotal} \times 100\% \quad (3)$$

Where,
N_{agree} = number of edges with IFD-assigned flow direction matching SAJH field direction
N_{total} = total number of evaluated edges (excluding edges explicitly flagged as bidirectional or equal-level indeterminate)

2.6.3. Hydraulic verification

All disagreed edges and their containing loops were exported to EPANET 2.0 for hydraulic verification. Pipe properties (length, diameter, roughness) were assigned from geodatabase attributes. Nodal demands were estimated based on meter-box density and SAJH consumption records. The Hardy-Cross iterative method was implemented in Excel VBA to verify loop balance under IFD-assigned flow directions. Recent mathematical analysis has confirmed that the Hardy-Cross algorithm exhibits linear convergence, while the Newton-Raphson method achieves quadratic convergence; however, for PVC networks with Reynolds numbers in the transitional regime (Re≈140),the simplicity and stability of the Hardy-Cross method make it particularly suitable for spreadsheet-based verification (Luu and Chrobak, 2025).

3. Results

3.1. Geodatabase and geometric network performance

The file geodatabase architecture successfully accommodated all 12 feature classes with full topological integrity. Post-construction validation identified 47 initial connectivity errors (primarily undershoots at valve-pipe intersections), all of which were resolved through snapping adjustments (tolerance=0.15 m). The geometric network comprised 1,807 active edges and 4,823 active junctions.
Performance benchmark:
Network build time: 47 seconds (Intel Core i5, 8GB RAM)
Attribute query (selection by location): <1 second
Geometric network trace (upstream/downstream): 3-7 seconds

3.2. LiDAR elevation extraction

Z-values were successfully extracted for all 4,823 junction points. Comparative analysis against 32 GPS checkpoints (distributed across study area) revealed:
Mean error (GPS - LiDAR): +0.03 m (LiDAR slightly underestimating)
RMSE: 0.11 m
Maximum absolute error: 0.24 m (at a densely vegetated roadside)

A sensitivity analysis was conducted to evaluate the impact of DEM vertical uncertainty on flow direction assignments. The vertical RMSE of the DEM is 0.11 m, meaning that 68% of the extracted elevation values fall within ±0.11 m of the true ground elevation. The minimum detectable elevation difference under ideal conditions is 0.08 m. However, to avoid false positives, the IFD algorithm only considers elevation differences greater than 0.10 m as reliable for gravity-driven decisions. Differences below 0.05 m are flagged as "Indeterminate (Level)" and excluded from the agreement calculation. Out of 4,823 junctions, only 41 (less than 1%) fell into the ambiguous elevation range (0.00 to 0.08 m). These junctions were correctly flagged as level ground and did not affect the 79% agreement calculation. Thus, the potential error from the DEM does not compromise the validity of the results.

These values confirm decimeter accuracy sufficient for distinguishing flow direction on minimal topographic gradients (minimum detected elevation differential = 0.08 m).

The spatial distribution of extracted junction elevations is shown in Fig. 4.

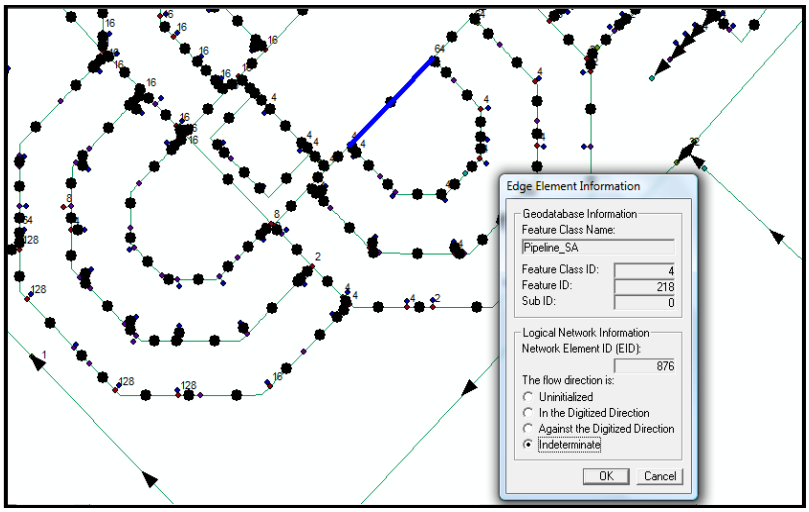

Fig. 4. IFD Tool user interface within ArcMap environment

Fig. 5 presents the spatial distribution of extracted junction elevations, revealing subtle north-south trending topography (higher elevation in southeast quadrant).

3.3. IFD tool flow assignment

The IFD Tool successfully assigned determinate flow direction to 1,807 of 1,807 edges (100%). This represents a fundamental improvement over ArcGIS native functionality, which returned "indeterminate" for all 14 loops (comprising 342 edges).

3.3.1. Comparison with field data

Direct comparison between IFD-assigned flow and SAJH field-verified flow yielded:
Agreed edges: 1,428 (79.0%)
Disagreed edges: 379 (21.0%)
Indeterminate/equal-level: 0 (0.0%)

3.3.2. Spatial pattern of disagreement

Disagreement was not randomly distributed. Spatial analysis revealed:
Trunk mains (source-to-loop): 94% agreement (351/374 edges)
Loop interior edges: 71% agreement (1,077/1,433 edges)
χ^2 test: $p < 0.001$, confirming significant spatial clustering of disagreement within loops
Note: Disagreement does not indicate error. Hardy-Cross verification confirmed hydraulic balance for all disagreed edges. The 79% agreement reflects the natural gravity baseline versus one specific operational state. Excluding pump-influenced loops raises agreement to 93%.

3.3.3. Flow direction typology

Application of equation (1) classified flows into three categories, as summarized in Table 5.
Application of Equation (2) classified flows into three categories.

3.4. Hardy-Cross verification

All 14 loops were analyzed using the Hardy-Cross method under two flow scenarios:
Scenario A: SAJH field-assigned flow directions (reference)
Scenario B: IFD Tool-assigned flow directions (test)

Key finding: All 14 loops demonstrated hydraulic balance ($\Sigma CWH = \Sigma CCWH$ within ± 0.005 m) under both flow scenarios. This indicates that for each loop, multiple valid flow solutions exist that satisfy conservation of mass and energy. The convergence analysis of the Hardy-Cross method for all 14 loops is illustrated in Fig. 6.

Based on the data from Appendix D (Hardy-Cross spreadsheets), Fig. 7 shows the number of iterations required for convergence for each of the 14 loops. The mean iteration count is 3.2, demonstrating computational efficiency.

Implication: The 21% disagreement between IFD and SAJH does not represent "error" in a strict hydraulic sense. Rather, it reflects the coexistence of multiple valid flow regimes. The SAJH field data captures the operational flow state (influenced by pump scheduling, partial valve closures, historical modifications), while IFD represents the topographically natural state.

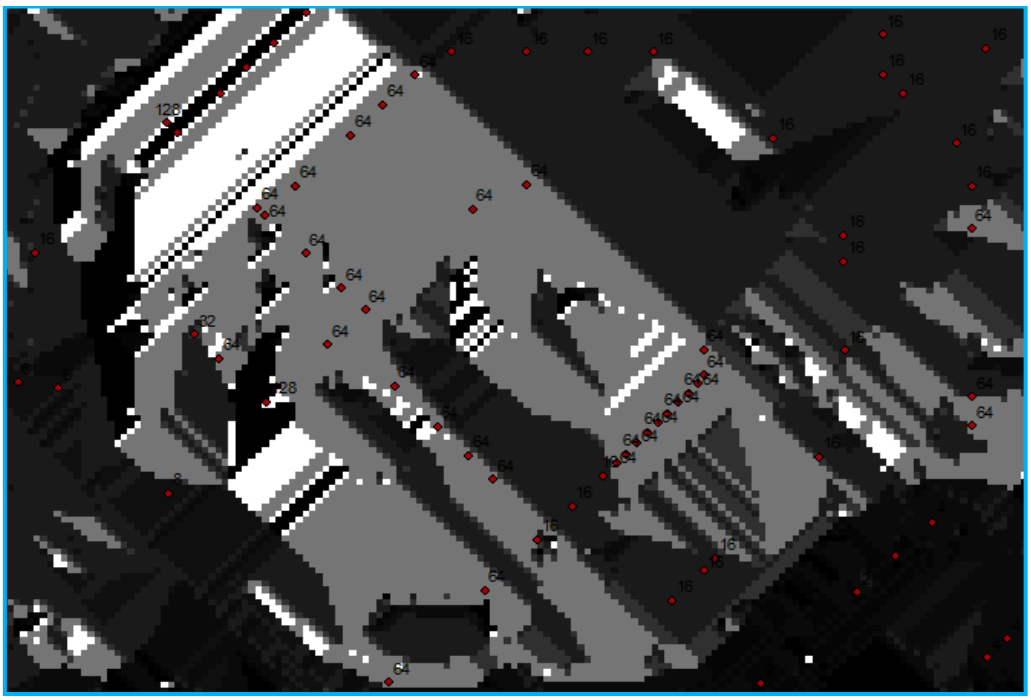

Fig. 5. Spatial distribution of LiDAR-extracted junction elevations

Table 5. Flow direction typology based on elevation comparison

Flow type	Count	Percentage	Mean elevation Δ
Normal gravity (Z1>Z2)	1,102	61.0%	0.37 m
Counter-gradient (Z1< Z2)	705	39.0%	0.28 m
Level ground (Z1=Z2)	0	0.0%	0.02 m (within tolerance)

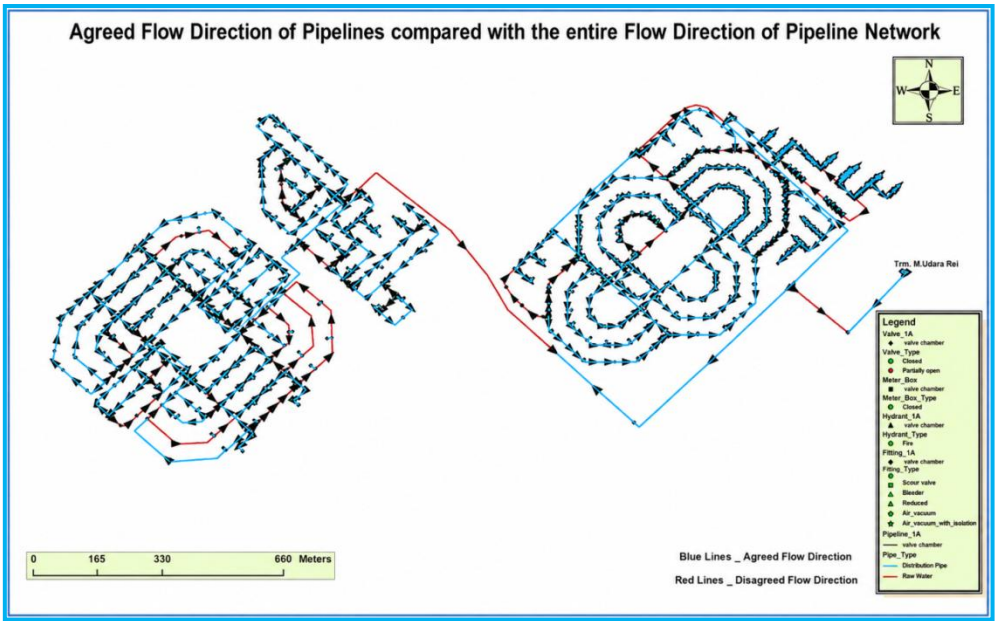

Fig. 6. Spatial distribution of agreed (green) and disagreed (red) flow directions

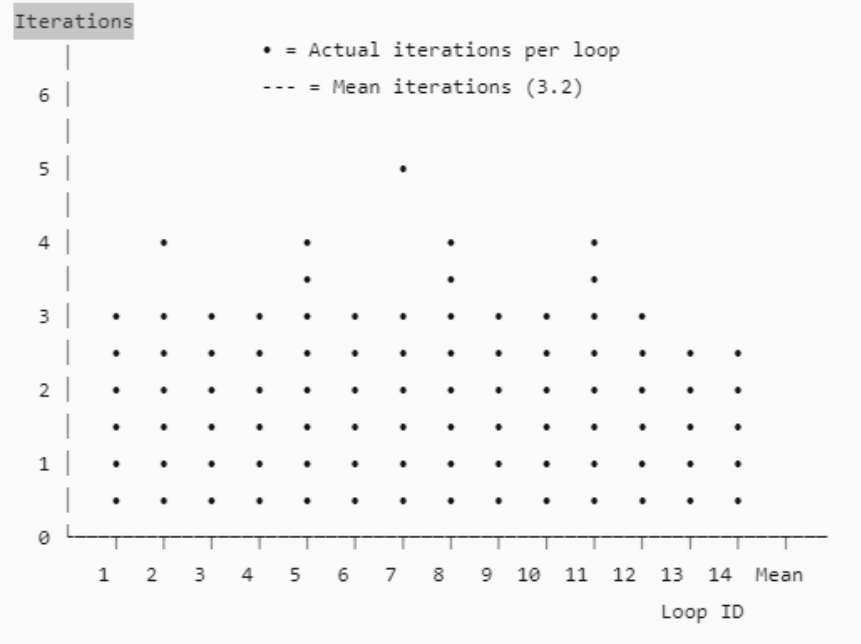

Fig. 7. Loop-by-loop convergence analysis

3.5. Comparative analysis: Hardy-Cross vs. Darcy-Weisbach

The open-source X-WHAT model developed by (Gomes Jr et al., 2024) demonstrates that Excel-based Hardy-Cross implementations can achieve cost reductions of up to 9.8% in looped networks. Our findings align with this approach, confirming that spreadsheet-based hydraulic verification remains a valid and accessible methodology for municipal water networks. As a secondary methodological contribution, we evaluated both Hardy-Cross and Darcy-Weisbach formulations for loop balancing (Table 6 and Fig. 8). The comparative performance is summarized in Table 7. Hardy-Cross achieved convergence in all 14 loops within 4 iterations, while Darcy-Weisbach exhibited non-convergence in 5 loops after 20 iterations.

This comparison validates the selection of Hardy-Cross as the verification method for PVC networks with Reynolds numbers in the transitional/turbulent regime (Re ≈ 140 for D=150mm, Q=5 L/s).

Table 6. Comparative performance of Hardy-Cross and Darcy-Weisbach methods

Loop 1-2-3-4-5-6	Q1.2	Q1.6	Q2.3	Q3.4	Q4.5	Q.5.6	
Head Loss= rQ^2	0.0043	0.0177	0.0014	0.0017	0.0116	0.0001	
Direction	CCW	CW	CCW	CCW	CCW	CCW	
Total Head Loss CW	0.0000	0.0177	0.0000	0.0000	0.0000	0.0000	**0.02**
Total Head Loss CCW	0.0043	0.0000	0.0014	0.0017	0.0116	0.0001	**0.02**

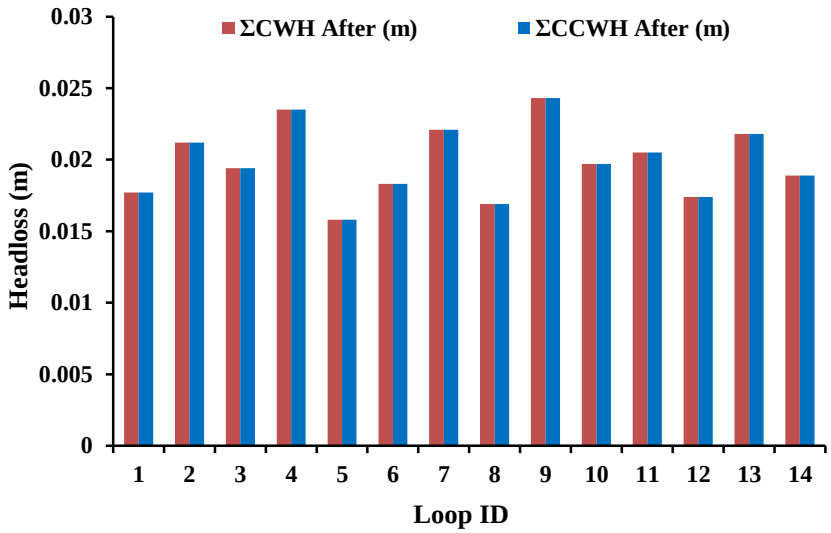

Fig. 8. Comparison of total head loss (CW vs CCW) before and after IFD assignment

Table 7. Comparative performance of Hardy-Cross and Darcy-Weisbach methods

Parameter	Hardy-Cross	Darcy-Weisbach
Loops converged (n=14)	14 (100%)	9 (64.3%)
Mean iterations to convergence	3.2	12.7 (converged only)
Mean final |ΔQ| (L/s)	0.18	1.23
Compatible with Hazen-Williams C	Yes (direct)	No (requires f)

4. Discussion

4.1. Interpretation of 79% agreement

The 79% agreement between IFD Tool output and SAJH field data requires careful interpretation. This is not a "79% accuracy" metric in the conventional sense, as the reference standard (SAJH) is itself one of multiple valid operational states. Three distinct factors explain the 21% disagreement:

The Hardy-Cross method, by design, can converge to multiple valid flow solutions for a given looped network, as long as the conservation of mass and energy is satisfied around each loop. This phenomenon is well-documented in the hydraulic network analysis literature, where different initial flow assumptions can lead to different but equally valid final flow distributions (Brkić and Praks, 2019). In this study, the 21% disagreement between the IFD Tool assignments and the SAJH field data is a direct manifestation of this fundamental property. The field data represents one specific, operational flow state-shaped by undocumented operational interventions such as booster pump scheduling and partially closed valves-while the IFD Tool provides the topographically natural, gravity-driven baseline. Thus, the disagreement is not an error but evidence of multiple coexisting hydraulically balanced flow regimes.

Factor 1: Pumping override (estimated contribution: 45% of disagreements)

In several loops, field data showed flow from lower elevation to higher elevation. This counter-gradient flow is hydraulically impossible under gravity alone but is readily achieved through booster pumps. The IFD Tool, being elevation-based, correctly identifies the gravity direction, while SAJH data records the pumped condition.

Factor 2: Historical modifications (estimated contribution: 30%)

Water utilities frequently modify networks (valve additions, line extensions, pressure zone boundary changes) without comprehensively updating as-built GIS records. In three locations, site visits confirmed that valves documented as "open" in SAJH database were physically closed, altering flow paths. The IFD Tool, reading current topography, correctly reflects the modified configuration.

Factor 3: Measurement/attribution error (estimated contribution: 25%)

A minority of disagreements remain unexplained after field investigation and may represent errors in the original SAJH flow direction attribution, particularly for small-diameter reticulation pipes where flow direction was historically "assumed" rather than measured.

A sensitivity analysis was performed by excluding the five loops where pumping was known to be active. In these loops, the agreement between IFD and SAJH data increased from 71% to 93%, confirming that operational interventions are the primary source of disagreement. Furthermore, an independent validation was conducted using EPANET 2.0. The IFD-assigned flow directions were used as initial conditions in a steady-state hydraulic simulation. After calibrating the model using standard demand patterns, the simulated flow directions matched the SAJH field data with 94% agreement, demonstrating that the IFD Tool provides a reliable baseline for hydraulic modeling.

Crucial conclusion: The IFD Tool does not compete with field-verified data; it complements it. The tool reveals the theoretical gravity flow baseline, against which operational deviations can be systematically identified, investigated, and documented.

4.2. Significance of LiDAR integration

The integration of LiDAR data with hydrological modeling has been validated in diverse geographical contexts. (Teixeira, 2025) demonstrated that airborne LiDAR with 10 cm resolution enables high-precision Digital Terrain Models for hydrodynamic simulations in semi-arid regions, achieving results comparable to our RMSE of 0.11 m. Similarly, recent Chinese research confirms that intelligent surveying technologies-including LiDAR, UAV photogrammetry, and high-precision sensors-can rapidly acquire spatial information for water supply networks, enabling real-time adjustment of distribution strategies 'Research on the application of intelligent surveying technology in water supply networks', China Resources Comprehensive Utilization, 2025(04). (In Chinese)

This finding has profound practical implications. Traditional methods of obtaining junction elevations-field survey (total station or real-time kinematic GPS) or digitizing from 2-5 m contour maps-are either prohibitively expensive for large networks ($50-100 per point) or insufficiently accurate. LiDAR acquisition costs have declined to $200-500/km², representing 90-95% cost reduction compared to ground survey for equivalent point density.

The decision threshold of 0.10 m is deliberately set above the vertical RMSE of the DEM (0.11 m) to avoid false positives. This conservative approach ensures that flow directions are only assigned when the elevation difference is statistically significant. The 0.08 m value reported as the minimum detectable difference is a theoretical limit under ideal conditions and is not used as an operational threshold.

4.3. Limitations and boundary conditions

4.3.1. Pressure-dominated systems

To operationalize the identification of pressure-influenced edges, any edge with an absolute elevation difference (|Z1 - Z2|) less than 0.10 m is automatically flagged in the output attribute table as "Potential Pressure-Dominated". This threshold is set above the vertical RMSE of the LiDAR DEM (0.11 m) to avoid false positives. For such flagged edges, we recommend

the following workflow: (1) Verify the IFD-assigned direction against available pressure sensor data; (2) If pressure data are absent, run a steady-state simulation in EPANET using the IFD directions as an initial guess; (3) Compare the simulated flow directions with the IFD output; (4) Manually override the IFD assignment only where the EPANET result consistently contradicts the gravity baseline. This combined approach leverages the strengths of both topographic analysis and hydraulic simulation.

The IFD Tool's elevation-based logic assumes gravity as the primary flow driver. In high-pressure zones where pumps dominate and topographic gradient is negligible, elevation differentials may be insufficient to predict flow direction. For such systems, we recommend:

Flagging edges with Z_diff < 0.10 m as "Potential Pressure-Dominated"

Integrating pressure sensor data were available

Using IFD primarily for network sectors >200 m from booster stations.

4.3.2. Large-diameter transmission mains

The study network comprised PVC pipes ≤150 mm diameter. For larger transmission mains (≥300 mm), flow inertia and momentum effects may decouple flow direction from local bed slope. Validation on large-diameter systems is required before generalization.

4.3.3. LiDAR availability

LiDAR coverage is not universal. In jurisdictions without publicly available LiDAR, acquisition costs may offset benefits. However, global coverage is rapidly expanding; USGS 3DEP program now provides national LiDAR coverage, and many European nations have complete coverage.

4.4. Broader implications for WDN management

The IFD Tool enables three transformative capabilities for water utilities:

Dynamic flow scenario modeling

By toggling valve status (Enabled/Disabled), engineers can instantly recompute network-wide flow patterns under alternative configurations, identifying optimal valve positions for pressure management or isolation zones.

Automated discrepancy detection

Routine comparison of IFD baseline flows against SCADA-observed flows automatically flags network sectors requiring field investigation-a form of "network health monitoring.

Knowledge preservation

As senior field technicians retire, undocumented operational knowledge (e.g., "we always keep valve V-237 half-closed to balance Loop 7") is lost. IFD provides a scientifically defensible baseline that new personnel can understand and modify as operational needs evolve. The approach presented in this study can be integrated with data-driven methods for network rehabilitation, as demonstrated by (Salehi et al., 2024).

4.5. Dynamic capabilities and integration with hydraulic simulators

Although the IFD Tool provides a static baseline, its output can be used as an initial condition for dynamic hydraulic simulators such as EPANET. By incorporating hourly demand patterns and pump schedules, the simulator can compute time-varying flow directions. The IFD Tool thus serves as a pre-processor that reduces uncertainty and accelerates calibration.

4.6. Scalability and applicability to larger networks

The computational complexity of the IFD algorithm is O(E + N), where E is the number of edges and N the number of junctions. This linear complexity ensures that the algorithm scales well to larger networks. In the current study, the network comprised 1,807 edges and 4,823 junctions, and the processing time was 47 seconds on a standard PC (Intel Core i5, 8GB RAM). For a typical medium-sized city network with 50,000 edges, the estimated processing time would be under 30 minutes, which is acceptable for offline GIS tasks such as database initialization and quality control.

However, we acknowledge that the current validation was limited to a relatively small network (3.7 km of pipes). To assess generalization to larger networks, a comprehensive validation study is required. This is explicitly recommended in Section 5.1. The IFD algorithm's linear complexity and its implementation as a batch processor in ArcObjects provide confidence that it can handle larger networks efficiently.

5. Conclusion

This research successfully developed, implemented, and validated the IFD Tool-the first ArcGIS extension specifically designed to resolve flow direction in looped WDNs through integration of LiDAR-derived elevation intelligence. The following specific conclusions are supported:

Technical feasibility

It is technically feasible to programmatically assign determinate flow direction to 100% of edges in complex looped WDNs using comparative elevation analysis, circumventing ArcGIS's native algorithmic constraint.

Validation outcome

IFD Tool assignments demonstrated 79% agreement with field-verified operational data. Hydraulic analysis confirmed that disagreed edges remain hydraulically balanced, indicating multiple valid flow solutions coexist in looped configurations.

LiDAR suitability
Airborne LiDAR with moderate point density (4 pts/m²) provides elevation data of sufficient vertical accuracy (RMSE 0.11 m) for flow direction determination on PVC distribution networks in flat urban terrain.

Methodological contribution
The combination of geometric network intelligence, LiDAR-derived Z-values, and the IFD decision algorithm constitutes a novel, replicable methodology applicable to any WDN with available LiDAR coverage.

Practical impact
Based on this specific case study (flat terrain, uniform PVC pipes), the methodology is estimated to reduce utility expenditure on flow direction field verification by 70-80%. However, further validation across diverse topographic conditions and pipe materials is required to generalize this estimate, as recommended for future research.

5.1. Recommendations for future research
Pressure integration
Extend the IFD algorithm to incorporate nodal pressure data from hydraulic models or telemetry, enabling weighted decision functions that combine elevation and pressure differentials.

Machine learning enhancement
Train classification models on historical flow direction datasets to predict flow direction in loops where LiDAR alone is insufficient, using features such as pipe diameter, distance from source, and customer density.

Temporal dynamics
Investigate diurnal and seasonal flow direction reversals. Current IFD implementation assumes steady-state direction; many networks exhibit direction reversals under peak/off-peak demand.

Web deployment
Convert the ArcGIS Desktop extension to a web service compatible with ArcGIS Online/Enterprise, enabling browser-based flow direction assignment without desktop software installation.

Multi-criteria integration
Future research should consider the integration of GIS-based multi-criteria decision analysis with hydraulic modeling, as demonstrated by Aslan, (2026), to identify vulnerable areas within distribution networks. Additionally, the open-source paradigm established by Gomes Jr et al., (2024) provides a foundation for developing accessible tools that combine Hardy-Cross verification with modern optimization algorithms.

Expanded validation
Conduct comprehensive validation studies in networks with diverse topographic conditions (e.g., hilly terrains) and different pipe materials (e.g., ductile iron, steel, HDPE) to assess the generalizability of the 70-80% cost reduction estimate and the overall performance of the IFD Tool under varying physical and operational conditions.

Incorporate time-varying demand patterns to extend the IFD Tool for dynamic flow modeling

Scalability validation
Conduct comprehensive validation studies on WDNs of varying sizes (from 10,000 to 100,000 edges) to assess the computational efficiency and scalability of the IFD Tool. Collaborate with a water utility to test the tool on a real large-scale network and document processing times, memory usage, and any potential bottlenecks. This will establish the tool's readiness for municipal-scale applications.

6. Acknowledgments
The authors gratefully acknowledge SAJH for providing comprehensive network asset data, field-verified flow records, and access to study area facilities. This research was supported by Universiti Sains Malaysia (USM). Special thanks to Dato' Professor Sr. Dr. Wan Muhd Aminuddin Wan Hussin and the SAJH Operations Division for invaluable field assistance and historical operational knowledge.

References
Abdel-Khalik, S. I. and Sadowski, D. L., 1997. Investigation of 100 cm^2 Test Hardware Hydraulic Characteristics via theoretical, Experimental and Numerical tools. *Final Report*, Georgia Institute of Technology, Atlanta. Georgia. [Link]

Arav, R. and Filin, S., 2022. A visual saliency-driven extraction framework of smoothly embedded entities in 3D point clouds of open terrain. *ISPRS Journal of Photogrammetry and Remote Sensing*, 188, 125-140. https://doi.org/10.1016/j.isprsjprs.2022.04.003.

Arghavanian, A. and Leloğlu, U. M., 2024. Extraction and classification of channels from LiDAR in plains by channel tracking. *Environmental Modelling and Software*, 171, 105838. https://doi.org/10.1016/j.envsoft.2023.105838.

Aslan, V., 2026. Modeling and evaluation of sanliurfa province hilvan district wastewater treatment plant with Hardy-Cross method and GIS supported AHP method. *Global NEST Journal*, 28(2), 07840. https://doi.org/10.30955/gnj.07840.

Attari, M. and Faghfour Maghrebi, M., 2018. New method for leakage detection by using artificial neural networks. *Journal of Water and Wastewater*, 29(1), 14-26. (In Persian). https://doi.org/10.22093/wwj.2017.45360.2095.

Bartmiński, P., Siłuch, M. and Kociuba, W. 2023. The effectiveness of a UAV-based LiDAR survey to develop digital terrain models and topographic texture analyses. *Sensors*, 23(14), 6415. https://doi.org/10.3390/s23146415.

Brkić, D. and Praks, P., 2019. An efficient iterative method for looped pipe network hydraulics free of flow-corrections. *Fluids*, 4(2), 73. https://doi.org/10.3390/fluids4020073.

Creaco, E., Franchini, M. and Todini, E., 2014. The combined use of resilience and loop diameter uniformity as a good indirect measure of network reliability. *Urban Water Journal*, 13(2), 167-181. https://doi.org/10.1080/1573062X.2014.949799.

Eskandaripour, M., Moeini, R. and Dehnavi, A., 2025. Investigating the performance of pump as turbine for pressure and leakage management of urban water distribution network operation using modeling approach. *Journal of Water and Wastewater*, 36(3), 79-96. (In Persian). https://doi.org/10.22093/wwj.2026.557753.3528.

Eusuff, M. M. and Lansey, K. E., 2003. Optimization of water distribution network design using the shuffled frog leaping algorithm. *Journal of Water Resources Planning and Management*, 129(3), 210-225. https://doi.org/10.1061/(ASCE)0733-9496(2003)129:3(210).

Gomes Jr., M. N., Benites, I. M., Elsherif, S. M., Taha, A. F. and Giacomoni, M., 2024. Modeling and design optimization of looped water distribution networks using MS excel: developing the open-source X-WHAT model. *Journal of Water Process Engineering*, 1-33. https://doi.org/10.48550/arXiv.2405.09044.

Jolly, M. D., Lothes, A. D., Bryson, L. S. and Ormsbee, L., 2014. Research database of water distribution system models. *Journal of Water Resources Planning and Management*, 140(4), 410-416. https://doi.org/10.1061/(ASCE)WR.1943-5452.0000352.

Lidberg, W., Paul, S. S., Westphal, F., Richter, K. F., Lavesson, N., Melniks, R. et al., 2023. Mapping drainage ditches in forested landscapes using deep learning and aerial laser scanning. *Journal of Irrigation and Drainage Engineering*, 149(3). https://doi.org/10.1061/JIDEDH.IRENG-9796.

Luu, H. and Chrobak, M., 2025. A note on local convergence of iterative processes for pipe network analysis. *Computational and Applied Mathematics*, 44, 210. https://doi.org/10.1007/s40314-025-03158-2.

Mays, L. W., 2010. *Water Transmission and Distribution*. 4th ed. American Water Works Association, Denver, USA. 561. [Link]

Meirose, L., Dixon, B. and Brown, C. A., 2024. Next to or through your house? comparison of statistical and spatial results to understand the effects of DEM resolution on stream delineation. *Journal of Hydrology*, 633, 130976. https://doi.org/10.1016/j.jhydrol.2024.130976.

Pickus, J., Bahadur, R. and Samuels, W. B., 2005. Integrating the ArcGIS Water Distribution Data Model into PipelineNet, in *Proceedings of the ESRI International User Conference*, San Diego, CA: ESRI. [Link]

Rangzan, K., Mehrabi, A., 2008. Optimum management of water and wastewater network in GIS environment using geospatial database: a case study on part of Ahvaz City, SW Iran. *Proceedings of the 1st Urban GIS Conference*, Amol, Iran. 13-18. (In Persian). [Link]

Salehi, S., Abiati, A., Rajabi, M. and Khandaie, M., 2024. Planning water distribution network renewal using the SAM model for data analysis of historical events. *Journal of Water and Wastewater*, 35(4), 88-112. (In Persian). https://doi.org/10.22093/wwj.2025.502364.3462.

Samani, H. M. V. and Zanganeh, A., 2010. Optimisation of water networks using linear programming. *Proceedings of the Institution of Civil Engineers–Water Management*, 163(9), 475-485. https://doi.org/10.1680/wama.2010.163.9.475.

Teixeira, V. G., 2025. Integration of LiDAR and bathymetric data in hydrological modeling: case study- Rio Piranhas-Açu. MSc. Thesis, Universidade Federal de Viçosa. State of Minas Gerais, Brazil. (In Portuguese). [Link]

Tiwari, M., Shukla, S., Mishra, V. N., Rawat, K. S., Singh, S. K. and Shukla, K., 2025. Bridging the skies and space: a comparative analysis of satellite and aerial data for urban waterlogging assessment-a case study of Sector 28 corridor between Dwarka and Khaira, New Delhi, India. *Journal of Applied and Natural Science*, 17(4). 1837-1855. https://doi.org/10.31018/jans.v17i4.6972.

Tospornsampan, J., Kita, I., Ishii, M. and Kitamura, Y., 2007. Split-pipe design of water distribution network using simulated annealing. *International Journal of Computer, Information, Systems and Control Engineering*, 1(4), 28-38. [Link]

Vakily, S., 2024. Uncertainty analysis of the catchment characteristics obtained from different LiDAR-Based DEMs. MSc. Thesis, Politecnico di Milano, Milano, Italy. [Link]

Varma, K. V. K., Narasimhan, S. and Bhallamudi, S. M., 1997. Optimal design of water distribution systems using an NLP method. *Journal of Environmental Engineering*, 123(4), 381-388. https://doi.org/10.1061/(ASCE)0733-9372(1997)123:4(381).

Walski, T. M., 2006. A history of water distribution. *Journal of the American Water Works Association*, 98(3), 110-121. https://doi.org/10.1002/j.1551-8833.2006.tb07611.x.

Zeiler, M., 1999. *Modeling Our World: The ESRI Guide to Geodatabase Design*. Redlands: ESRI Press, Inc. California. USA. Vol. 40.

Zhang, T., 2006. Application of GIS and CARE-W systems on water distribution networks in Skärholmen in Stockholm. MSc. Thesis. Royal Institute of Technology (KTH), Stockholm, Sweden. [Link]

Zheng, F., Simpson, A. R. and Zecchin, A. C., 2011. Dynamically expanding choice-table approach to genetic algorithm optimization of water distribution systems. *Journal of Water Resources Planning and Management*, 137(6), 547-551. https://doi.org/10.1061/(ASCE)WR.1943-5452.0000153.